Low-cost high-performance fiber-optic pH sensor based on thin-core fiber modal interferometer

Bobo Gu[1], Ming-Jie Yin[2], A. Ping Zhang[1]*, Jin-Wen Qian[2], and Sailing He[1,3]

[1]*Center for Optical and Electromagnetic Research, State Key Laboratory of Modern Optical Instrumentation, Zhejiang University, Hangzhou 310058, China*

[2]*Department of Polymer Science and Engineering, Key Laboratory of Macromolecule Synthesis and Functionalization (Ministry of Education), Zhejiang University, Hangzhou 310027, China*

[3]*Division of Electromagnetic Engineering, School of Electrical Engineering, Royal Institute of Technology, S-100 44 Stockholm, Sweden*

**zhangap@zju.edu.cn*

Abstract: A new fiber-optic pH sensor based on a thin-core fiber modal interferometer with electrostatic self-assembled nanocoating is presented. After inserting a segment of thin-core fiber into a standard single-mode fiber, high-order cladding modes are excited and interfere with the core mode to form an in-fiber modal interferometer. The side surface of the sensor is then deposited with poly(allylamine hydrochloride) and poly(acrylic acid) nanocoating by electrostatic self-assembly technique. A fast and linear response is obtained in either acid or alkali solution (in the pH range 2.5 to 10) with resolution of 0.013 pH unit.

OCIS codes: (060.2370) Fiber optics sensors; (060.2340) Fiber optics components.

References and links

1. H. Lehmann, G. Schwotzer, P. Czerney, and G. J. Mohr, "Fiber-optic pH meter using NIR dye," Sens. Actuators B Chem. **29**(1–3), 392–400 (1995).
2. P. A. Wallace, N. Elliott, M. Uttamlal, A. S. Holmes-Smith, and M. Campbell, "Development of a quasi-distributed optical fibre pH sensor using a covalently bound indicator," Meas. Sci. Technol. **12**(7), 882–886 (2001).
3. O. B. Miled, A. B. Ouada, and J. Livage, "pH sensor based on a detection sol–gel layer onto optical fiber," Mater. Sci. Eng. C **21**(1–2), 183–188 (2002).
4. N. K. Sharma, and B. D. Gupta, "Fabrication and characterization of a fiber-optic pH sensor for the pH range 2 to 13," Fiber Int. Opt. **23**(4), 327–335 (2004).
5. J. Goicoechea, C. R. Zamarreño, I. R. Matías, and F. J. Arregui, "Optical fiber pH sensors based on layer-by-layer electrostatic self-assembled neutral red," Sens. Actuators B Chem. **132**(1), 305–311 (2008).
6. X. H. Yang, and L. L. Wang, "Fluorescence pH probe based on microstructured polymer optical fiber," Opt. Express **15**(25), 16478–16483 (2007), http://www.opticsinfobase.org/abstract.cfm?URI=oe-15-25-16478.
7. A. Safavi, and M. Bagheri, "Novel optical pH sensor for high and low pH values," Sens. Actuators B Chem. **90**(1–3), 143–150 (2003).
8. B. D. Gupta, and S. Sharma, "A long-range fiber optic pH sensor prepared by dye doped sol-gel immobilization technique," Opt. Commun. **154**(5–6), 282–284 (1998).
9. B. D. Gupta, and S. Sharma, "Fabrication and characterization of pH sensor based on side polished single mode optical fiber," Opt. Commun. **216**(4–6), 299–303 (2002).
10. S. Dong, M. Luo, G. Peng, and W. Cheng, "Broad range pH sensor based on sol–gel entrapped indicators on fibre optic," Sens. Actuators B Chem. **129**(1), 94–98 (2008).
11. R. B. Thompson, and J. R. Lakowicz, "Fiber optic pH sensor based on phase fluorescence lifetimes," Anal. Chem. **65**(7), 853–856 (1993).
12. W. C. Michie, B. Culshaw, M. Konstantaki, I. McKenzie, S. Kelly, N. B. Graham, and C. Moran, "Distributed pH and water detection using fiber-optic sensors and hydrogels," J. Lightwave Technol. **13**(7), 1415–1420 (1995).
13. J. Goicoechea, C. R. Zamarreño, I. R. Matías, and F. J. Arregui, "Utilization of white light interferometry in pH sensing applications by mean of the fabrication of nanostructured cavities," Sens. Actuators B Chem. **138**(2), 613–618 (2009).
14. J. M. Corres, I. del Villar, I. R. Matias, and F. J. Arregui, "Fiber-optic pH-sensors in long-period fiber gratings using electrostatic self-assembly," Opt. Lett. **32**(1), 29–31 (2007).

#118467 - $15.00 USD Received 12 Oct 2009; revised 17 Nov 2009; accepted 17 Nov 2009; published 23 Nov 2009

15. J. M. Corres, I. R. Matias, I. del Villar, and F. J. Arregui, "Design of pH Sensors in long-period fiber gratings using polymeric nanocoatings," IEEE Sens. J. **7**(3), 455–463 (2007).
16. A. P. Zhang, L. Y. Shao, J. F. Ding, and S. He, "Sandwiched long-period gratings for simultaneous measurement of refractive index and temperature," IEEE Photon. Technol. Lett. **17**(11), 2397–2399 (2005).
17. M. Jiang, A. P. Zhang, Y.-C. Wang, H. Y. Tam, and S. He, "Fabrication of a compact reflective long-period grating sensor with a cladding-mode-selective fiber end-face mirror," Opt. Express **17**(20), 17976–17982 (2009), http://www.opticsinfobase.org/oe/abstract.cfm?uri=oe-17-20-17976.
18. P. Zhang, J. W. Qian, Q. F. An, B. Y. Du, X. Q. Liu, and Q. Zhao, "Influences of solution property and charge density on the self-assembly behavior of water-insoluble polyelectrolyte sulfonated poly(sulphone) sodium salts," Langmuir **24**(5), 2110–2117 (2008).
19. Q. Zhao, J. W. Qian, Q. F. An, and B. Y. Du, "Speedy fabrication of free-standing layer-by-layer multilayer films by using polyelectrolyte complex particles as building blocks," J. Mater. Chem. (2009), doi:10.1039/b911386j.
20. K. Itano, J. Choi, and M. F. Rubner, "Mechanism of the pH-induced discontinuous swelling/deswelling transitions of poly(allylamine hydrochloride)-containing polyelectrolyte multilayer films," Macromolecules **38**(8), 3450–3460 (2005).

1. Introduction

Optical biochemical sensors are under rapid development because of their important applications in environmental monitoring and clinical analysis. Among various types of biochemical sensors, the pH sensor is one of the most essential sensors because of the importance of pH control or measurement in numerous fields, e.g., biology, clinical medicine, ecology, etc. Although the titration method has been used for long time, the development of miniaturized optical pH sensor is still a very active research topic. In recent years, fiber-optic pH sensors have attracted increasing interests due to their many advantages, such as small size, remote sensing capability, and the safety for in vivo measurement.

Several types of fiber-optic pH sensors were proposed and demonstrated [1–15]. One type of fiber-optic pH sensor is based on pH indicator immobilized in the matrix materials. The pH indicators that have been proposed include acidochrome dye [1], fluorescein acrylamide [2], thymol blue [3], ethyl violet dye [4],neutral red [5], eosin [6], the mixture of dipicrylamine and victoria blue [7], or the mixture of cresol red, bromophenol blue and chlorophenol red [8-10]. The optical properties of the indicators, including absorbance [1, 3–5,7–10], fluorescent intensities [2, 6], and fluorescent lifetime [11], can be employed for the determination of the pH of the liquid under test. The other type of fiber-optic pH sensor is based on the morphology of nanostructured film, usually known as swelling. Since the refractive index (RI) of a swellable film, e.g. hydrogel [12] or polyelectrolyte-deposited nanostructured material [13–15], depends on the pH, one can design pH sensors through the measurement of external RI. Since most of the pH indicators work in UV-visible range, while most of fiber-optic components work in near-infrared range, a fiber-optic pH sensor based on swellable film is competitive because of the compatibility with fiber-optic sensor networks and the robustness of the sensor [13–15]. The absorption or fluorescence-based pH sensors have some inherent drawbacks since they are influenced by light intensity fluctuations, temperature, and concentration of indicator. The avoidance of the indicator can solve well the deterioration issues induced by bleaching or leaching of the indicator to make a long-term fiber-optic sensor for on-line pH monitoring applications.

In order to realize a reliable and accurate measurement of the RI of the nanostructured film for pH sensing, several pH sensing schemes based on the resonant optical responses have been recently proposed and demonstrated [13–15]. Corres *et al.* presented a long-period grating (LPG) pH sensor, in which nanocoating was deposited on the side-surface of the LPG as the reacting functional film and the shift of the resonant wavelength of the LPG is utilized for the determination of pH-induced RI changes. Goicoechea *et al.* demonstrated a Fabry-Perot (FP) nanocavity pH sensor, in which the nanostructured film was prepared on the fiber-end surface and the white-light interferometry is employed for the measurement of pH induced swelling of the film. The electrostatic self-assembly (ESA) deposition technique was used for the film preparation in both of the above-mentioned works because the ESA has high controllability and repeatability on organic or inorganic nanocoating preparation.

#118467 - $15.00 USD Received 12 Oct 2009; revised 17 Nov 2009; accepted 17 Nov 2009; published 23 Nov 2009

In this paper, we propose a new fiber-optic pH sensor based on fiber modal interferometer (FMI). The fiber device has a short segment of thin-core fiber (TCF) inserted into a standard single-mode fiber (SMF). After nanocoating the FMI with ESA deposition method, the FMI can be used for pH sensing. The basic structure and even the spectrum of this sensor are very similar to those of an LPG sensor. However, the present sensor has not only a slightly higher sensitivity to external RI, but also much lower sensitivity to temperature. Moreover, it has the advantages of the robustness (because of the avoidance of grating degradation issue) and the lower fabrication cost.

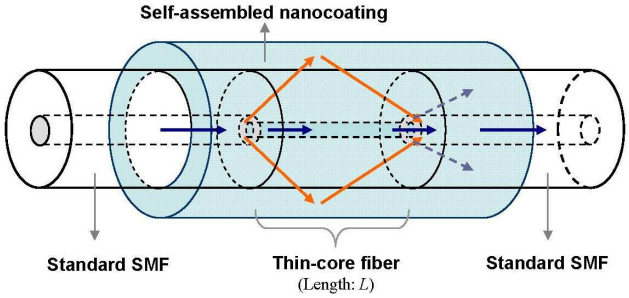

Fig. 1. Schematic configuration of the fiber-optic pH sensor based on thin-core fiber interferometer (TCFMI) with electrostatic self-assembled nanocoating.

2. Thin-core fiber modal interferometer

Figure 1 shows the schematic configuration of the thin-core fiber modal interferometer (TCFMI) we propose. It is different from an LPG, and high-order fiber cladding modes are excited not by resonant scattering, but by mode mismatch at the starting point of the TCFMI. The excited cladding modes will interfere with the core mode and form some local maxima or minima because of the constructively or deconstructively interference, respectively. If one pays attention to a local minimum at the ending point, which results a dip in the transmission spectrum, the relative phase displacement of the interfering two modes can be described as

$$2\pi\,[n_{eff}^{co}(\lambda)-n_{eff}^{cl,j}(\lambda,n_{ext})]\frac{L}{\lambda_D}=(2k+1)\pi\,, \tag{1}$$

where n_{eff}^{co} is the effective index of the core mode, $n_{eff}^{cl,j}$ is the effective index of the j-th order cladding mode, n_{ext} is the RI of the surrounding medium, L is the length of the inserted fiber, λ_D is the wavelength of the transmission dip, and k is an integer. Since the effective index of the cladding mode depends on the external RI, the transmission dip will shift if the external RI is changed. The sensitivity of the transmission dip to the change of external RI and the temperature can be deduced from Eq. (1) as

$$\frac{d\lambda_D}{d\,n_{ext}}=\frac{-\lambda_D}{\Delta n_{eff}}\frac{\partial n_{eff}^{cl,j}}{\partial n_{ext}}/[1-\frac{\lambda_D}{\Delta n_{eff}}(\frac{\partial n_{eff}^{co}}{\partial\lambda}-\frac{\partial n_{eff}^{cl,j}}{\partial\lambda})]\,, \tag{2.a}$$

$$\frac{d\lambda_D}{dT}\cong[\frac{\lambda_D}{\Delta n_{eff}}(\frac{\partial\Delta n_{eff}}{\partial n_{co}}\frac{dn_{co}}{dT}+\frac{\partial\Delta n_{eff}}{\partial n_{cl}}\frac{dn_{cl}}{dT})+\frac{\lambda_D}{L}\frac{dL}{dT}]/(1-\frac{\lambda_D}{\Delta n_{eff}}\frac{\partial n_{eff}}{\partial\lambda})\,, \tag{2.b}$$

where Δn_{eff} is the difference of the effective indices of the core mode and the cladding mode, n_{co} is the RI of the core, and n_{cl} is the RI of the cladding.

The TCFMI sensor was fabricated by using a commercial thin-core optical fiber (Nufern 460-HP). The core diameter of the fiber is ~3.0 μm, and the cutoff wavelength is ~450 nm.

#118467 - $15.00 USD Received 12 Oct 2009; revised 17 Nov 2009; accepted 17 Nov 2009; published 23 Nov 2009

Figure 2(a) shows the spectrum responses of the fabricated TCFMI with 2 cm long TCF when the external RI changes. After immersing into the glycerol/deionized-water solution, the transmission dip of the TCFMI shifts to longer wavelength with the sensitivity of 138 nm/R.I.U. The samples under test are glycerol solutions with concentration (volume %) of 0, 0.40, 2.45, 5.06, 7.84, 12.91, 19.82, 37.3, and 62.3%, whose RIs are 1.333, 1.3336, 1.3365, 1.34, 1.3436, 1.3496, 1.3572, 1.373 and 1.3897, respectively. Comparing with the previously reported LPG sensors [14–17], one can see that their sensitivities to external RI are comparable to each other, but the transmission dip of the TCFMI shift to the opposite direction. This is because the cladding mode in the TCF satisfies $(\partial n_{eff}^{co} / \partial \lambda - \partial n_{eff}^{cl,j} / \partial \lambda) > \Delta n_{eff} / \lambda_D$ as one can see from Eq. (2.a).

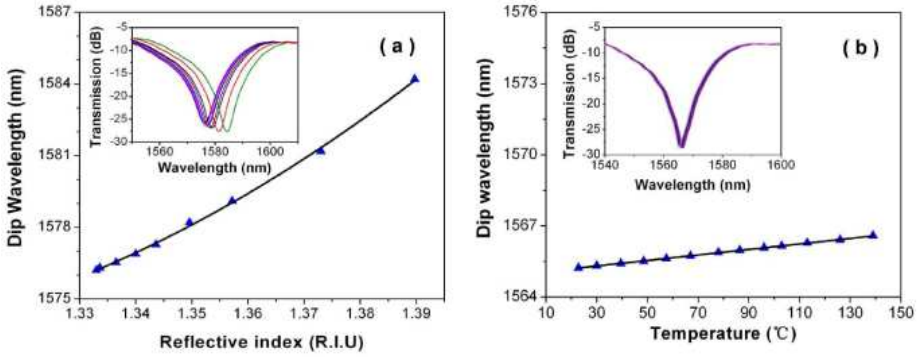

Fig. 2. The spectral responses of the TCFMI to the change of external refractive-index (a) and temperature (b). The insets show the measured transmission spectra.

Figure 2(b) shows the temperature response of the TCFMI, which is measured by using a temperature-controlled oven. The transmission dip is observed to shift to longer wavelength with increasing of temperature, which is also opposite to the temperature response of normal LPG sensors. The measured temperature sensitivity is 0.012 nm/°C, which is about a twentieth of that of conventional LPG sensor. The lower temperature sensitivity is a desirable merit for an RI sensor because of the suppression of the cross sensitivity to temperature.

3. Fabrication and characterization of TCFMI pH sensor

A nanocoating was deposited on the side surface of TCFMI by solution dipping layer-by-layer ESA technology [18] for pH sensing. The method is based on the construction of molecular multi-layers by the electrostatic attraction between oppositely charged polyelectrolyte. Poly(allylamine hydrochloride) (PAH) and poly(acrylic acid) (PAA) were utilized as the cationic and anionic materials in the experiment. All chemicals are purchased from Sigma-Aldrich and used without further purification.

#118467 - $15.00 USD Received 12 Oct 2009; revised 17 Nov 2009; accepted 17 Nov 2009; published 23 Nov 2009

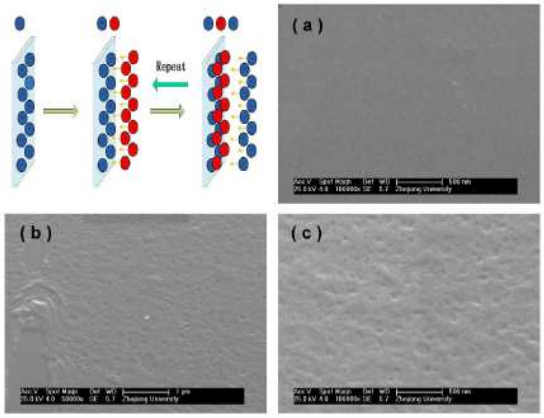

Fig. 3. Electrostatic self-assembly deposition process and the scanning electron microscopy images of the nanocoating: (a) the surface of optical fiber before ESA deposition; (b) and (c) images of the nanocoating with and without defects.

The ESA method is shown schematically on the left-up corner in Fig. 3. Both PAH and PAA were dissolved in 1M NaCl aqueous solution with concentration of 2 g/L. After cleaned by piranha solution (H_2SO_4 and H_2O_2 in concentration of 7:3), the TCFMI was washed with large amount of deionized water and dried by nitrogen gas. Therefore, the fiber surface is negatively charged [19]. The fiber was then immersed into PAH and PAA alternatively with reaction of 4 min to form a monolayer of polymer through electrostatic adsorption. After each monolayer was formed, the fiber was rinsed by deionized water for 1 min to remove the excess molecules. Each polycation/polyanion layer (PAH/PAA) is called a bilayer. After depositing 25 bilayers, the optical fiber was baked in an oven at 60 °C for 10 hours.

The deposited nanocoating was characterized by utilizing scanning electron microscopy (SEM). Figure 3(a) shows the SEM photos of the naked fiber surface, and Fig. 3(b) and Fig. 3(c) show the surface morphology of the nanocoating with different magniscales. Some local defects were observed in the image with small magniscale, as shown in Fig. 3(b). Meanwhile, it also shows that the nanocoating has a bumpy surface with nano-indents. The thickness of the nanocoating measured by the SEM is around 100 nm.

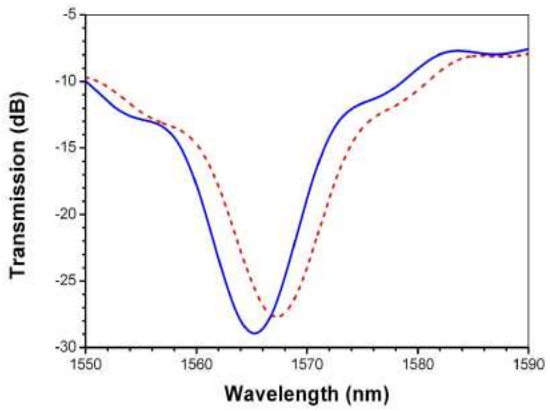

Fig. 4. The spectrum of the TCFMI before (solid line) and after (dashed line) the deposition of nanocoating.

The transmission spectra of the TCFMI before and after the nanocoating deposition were recorded by an optical spectrum analyzer (ANDO, AQ6317) for a comparison. As shown in Fig. 4, the fabricated TCFMI has a transmission dip at 1565 nm, resulting from a destructive

#118467 - $15.00 USD Received 12 Oct 2009; revised 17 Nov 2009; accepted 17 Nov 2009; published 23 Nov 2009

interference as discussed before. The transmission dip shifts to 1568 nm after the deposition of nanocoating. It attributes to the nanocoating induced changes of the effective index of the reacting cladding mode, since the temperature effect is neglectable in our measurement.

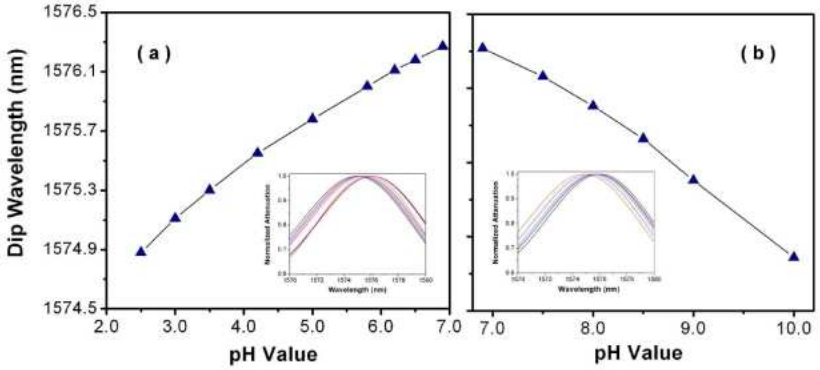

Fig. 5. The response of the fabricated TCFMI pH sensor to acidic (a) and alkaline (b) solutions. The insets show the measured spectra.

The fabricated TCFMI pH sensor was tested with HCl and NaOH aqueous solutions. The sensor was packaged with a shallow aluminum groove for the test. Figure 5 shows the spectral response of the sensor to different buffer solutions. One can see that the transmission dip shifts to shorter wavelength with decreasing of pH value in acidic range, and also shifts to shorter wavelength with increasing of pH value in alkaline range. This is because the ionization state of the PAH/PAA multi-layer is modulated by the pH value through swelling/deswelling and reaches maximum at the neutral pH [20]. The modulation of ionization state induces a change of the density of the polyelectrolyte nanocoating, which results a change of the RI of nanocoating. The sensitivities of the fabricated TCFMI pH sensor are 0.32 nm/pH unit and −0.45 nm/pH unit for acid and alkali solutions, respectively. The sensor can be alternatively used for either acid or alkali solution because the corresponding calibration curves is different in the two cases, which reduces the operating range of the sensor.

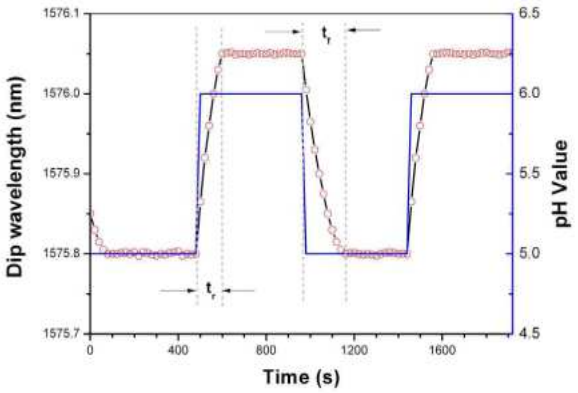

Fig. 6. The measured dynamic response of the TCFMI pH sensor.

The dynamic response of the pH sensor was also measured in the experiment. The optical spectrum analyzer keeps sweeping with period of 8 s. The buffer solutions with pH value of 5 and 6 are alternately added into the testing groove. As shown in Fig. 6, the rise time (t_r) of the sensor is 120 s and the fall time (t_f) is 200 s. The variation of dip wavelength for a given pH

#118467 - $15.00 USD Received 12 Oct 2009; revised 17 Nov 2009; accepted 17 Nov 2009; published 23 Nov 2009

value was measured as 0.004 nm. Since the wavelength sensitivity of the sensor is 0.3 nm/pH unit, one can deduce the effective resolution of the pH sensor as 0.013 pH unit.

4. Discussion and conclusion

We have presented a new type of fiber-optic pH sensor based on a TCF modal interferometer. The TCFMI has a regular spectrum with a high extinction-ratio transmission dip. Because of the resonant nature with the cladding mode, the transmission dip is highly sensitivity to external RI. Comparing to the well-know LPG-based RI sensor, the TCFMI has a comparable RI sensitivity and much lower temperature-sensitivity. A drawback of the sensor is the relatively high insertion loss, which was measured in the experiment as around 7 dB.

After depositing the side surface with PAH/PAA multi-layers by ESA technique, the TCFMI sensor has been used to measure acid and alkali solutions. Although some defects of nanocoating were observed by SEM imaging, as shown in Fig. 3(b), the sensor showed high performance on the pH measurement. The resolution of pH sensor is as high as 0.013 pH unit, thanks to the highly stable spectrum response of the sensor. It is also because the reacting side-surface of the fiber sensor is relatively large, and thus the requirement of defect control is not as rigorous as that of a fiber-optic pH sensor based on a fiber-end nanocavity.

The TCFMI sensor proposed in this paper has advantages of low-cost, robustness, reversibility, high sensitivity to external RI, and low temperature sensitivity, and is therefore very suitable for use as remote single-point monitoring biosensors or disposable low-cost fiber-optic bioprobes.

Acknowledgment

This work was supported by Natural Science Foundation of China (Grant No: 60607011 and 20876134) and Key Program of Natural Science Foundation of China (Grant No: 90101024).

#118467 - $15.00 USD Received 12 Oct 2009; revised 17 Nov 2009; accepted 17 Nov 2009; published 23 Nov 2009